CONVERGENT AND DIVERGENT ANGLES OF A SOLID-FUEL ROCKET NOZZLE AND ITS INFLUENCES ON THE MOTOR'S THRUST CURVE

G. A. J. Gonini,
A. Aliano,
L. T. Moresco,
LI. B. Pasquali,
and A. A. M. Oliveira Jr

Universidade Federal de Santa Catarina
Departamento de Engenharia Mecânica
Bairro Jardim das Américas
Florianópolis, Santa Catarina, Brasil
rudmar@ ufpr.br
gonini.gabriel@gmail.com
amanda.aliano@hotmail.com
luiza.ternes.moresco@gmail.com
isabrisot@gmail.com;
amir.oliveira@gmail.com

Received: Nov 03, 2022
Revised: Nov 08, 2022
Accepted: Nov 20, 2022

ABSTRACT

The main goal of this work is to investigate how the angles of a convergent-divergent rocket nozzle influence the thrust curve of a solid-propulsion rocket. The work has been conducted within an academic rocketry team. As there is not clear reasoning on how to define these angles, the present research provides insights on how these geometrical parameters influence the performance of a rocket motor. A 2D-axisymmetric CFD domain is considered, comprising the fluid domain inside and outside the nozzle, to give room for the shock waves to happen and also accommodate the flow. The study comprises a baseline geometry and twelve modified designs, varying the convergent and the divergent angles of the nozzle. Since the convergent diameter must match the chamber diameter, it is fixed. For the divergent diameter, there is no such restriction; therefore, there are two possibilities: a divergent section with the same divergent diameter orwith the same length as the baseline. The benchmark thrust curve is generated with a MATLAB code based on solid-fuelmodeling and the De Laval theory. The curve is divided into six steady-state simulations, using boundary conditions of mass flow, pressure and temperature at the inlet and pressure and temperature at the outlet. The baseline geometry is simulated in Ansys Fluent and normalized by the MATLAB benchmark. A mesh study selects which mesh and turbulence model to use based on this normalization. The modified geometries are then compared to the baseline. The main quantity of interest is the thrust but quantities such as static pressure and average velocity at the nozzle exit aid the understandingof the changes in thrust.

Keywords: convergent-divergent nozzle; thrust; propulsion; aerodynamics; rocketry

INTRODUCTION

During the last decade, the number of rocketry teams and aerospace competitions increased in Brazil and Latin America. In its most recent project, Apex Rocketry has developed a low-apogee single-stage solid-propelled rocket, the so- called Armação A-22 rocket. The purpose of the nozzle is to expel the burnt gases generated by the combustion of the solid propeller and generate thrust. The convergent-divergent conical configuration, as known as De Laval's nozzle, is vastly used in rocketry. Although the geometry is very simple, the complexity of the flow and the dependence upon fuel conditions does not provide a concrete answer regarding the ideal dimensions of the nozzle. Therefore, the objective of the present work is to investigate how the angles of a convergent-divergent rocket nozzle influence the thrust curve.

The convergent half-angle used in Armação A-22 is 28.5°, based on the results presented by Mir et al. (2017). Their study comprised geometries varying the convergent angle from 28° to 30° and keeping the same expansion ratio and boundary conditions, using a 2D axisymmetric domain, with a density-based coupled solver, under k-ω SST turbulence model. The nozzle, the mass flow rate and the pressure, however, are much higher than the ones used in rocketry.

The divergent half-angle used in Armação A-22 is 12° recommended by Sutton and Biblarz (2016). The authors describe a range of 10° to 12° for a divergent half-angle in conical nozzles as equivalent to the ideal bell-shaped nozzle (minimum loss), although they warn of the possibility of nozzles becoming too long. To respect the vehicle mass ratios, Apex Rocketry opted for the highest angle.

Noh et al. (2011) investigated smaller nozzles, compatible with rocketry scales, as the designs had divergence lengths from 22.1 to 62.9 mm (that corresponds to a range of 28° to 11° for the divergent half-angle) and a throat diameter of 11 mm. However, the thrust was very low (about 50 N), much lower than Armação's. The simulations considered a 2D axisymmetric domain, with a

coupled solver, under Spalart-Allmaras turbulence model.

Biju Kuttan and Sajesh (2013) also investigated the divergent angle, varying from 4° to 15° (4°, 7°, 10°, 13° and 15°). The scales of the problem, however, are too large for rocketry purposes. The simulations considered a 2D axisymmetric domain, with a density-based solver, under standard k-ε turbulence model. In their work, the increase in the divergent angle displaces the shock waves towards the exit of the nozzle. As it increased to 15°, the shock was completely eliminated from the nozzle and was considered as a good design.

Natta et al. (2012) considered a 2D-axisymmetric model to evaluate different divergent angles (7°, 20°, 30° and 40°), while maintaining a fixed exit diameter. They found out that the velocity at the exit increased as the divergent angle was increased. The turbulence intensity however increased and at the exit of the nozzle, at 40°, it was considered to be very high (5.75e+03%). They concluded that the efficiency of the nozzle increased as the divergent angle was increased, up to a certain extent.

Hamedi-Estakhrsar et al. (2018) is the only work presented in this literature review that considers the outside of the nozzle in the fluid domain. Furthermore, it considered different operating conditions and studied geometries with convergent half-angles of 5°, 10°, 20.84° (baseline), 30° and 40° and divergent half-angles of 5°, 10.85° (baseline), 20°, 30° and 40°, keeping throat and exit areas constant. They considered a 2D-axisymmetric domain, under the k-ω SST turbulence model. Their conclusions are based on some coefficients (discharge, velocity and gross thrust) and nozzle efficiency. For a convergent half-angle of 40°, there is flow separation. Concerning the divergent half-angle, it has no significant effects on the discharge coefficients.

ANALYTICAL BENCHMARK

The analytical performance prediction is made for a solid rocket propulsion system, using a MATLAB script. The results characterize the performance of a motor carrying four cylindrical grains with external surface inhibited (Bates grains). The core and external diameter dimensions are about 20 mm and 65 mm, respectively, and a length of 120 mm. The combustion chamber has an internal diameter of about 70 mm and 500 mm of free length. The nozzle is conical, convergent-divergent. The convergent section (inlet diameter) is equal to the combustion chamber dimension, with a half-angle of 28.5°, while the divergent section has a diameter nearly of 50 mm and a half-angle of 12°. The throat diameter is approximately 20 mm. The classification of the motor is L, based on its total impulse.

The De Laval theory is applied to analyze the flow through the nozzle, considered isentropic, i.e. reversible and adiabatic. The performance evaluation is divided into fixed periods to consider a permanent regime for each range of analysis, with the gas flowing along the same streamlines. The flow through the nozzle is one-dimensional and non- rotational. The gas flow behavior is compressible since the Mach number is greater than 0.3.

The solid propellant considered is KNDX, with the potassium nitrate being the oxidizer (O) and dextrose the fuel (F), in a proportion of 65/35 O/F. The propellant burning rate is a function of the combustion chamber pressure, propellant composition and conditions. The local burning-front progression rate is affected by mass flux, local static pressure, and grain temperature, Miller (1971). For propellants with a low mass flux in the grain cavity, the burning rate is expressed as a function of the stagnation chamber pressure value (P_0, in MPa), as shown in Eq. (1).

$$r = a P_0^n \tag{1}$$

with r being the linear burning rate of the propellant, in mm/s; a the coefficient of pressure and n the linear burning rate pressure exponent. The coefficient a and n exponent are functions of pressure and evaluated based on experiments.

The burning causes variation in grain dimensions generating combustion gases. In this analysis, the circumferential burning-front is neglected, the external surface of the grain is considered inhibited and it assumes that all non-inhibited surfaces are ignited at the same time. The combustion gases provide an increase in the chamber pressure and in the mass flow rate until the blocked state is reached, Eq. (2).

$$\dot{m}_{max} = \left[\frac{2}{k_m + 1}\right]^{\frac{k_m+1}{2(k_m-1)}} A_e P_0 \sqrt{\frac{k_m}{RT_0}} \tag{2}$$

with k_m as the ratio of specific heats for mixture, A_e the exit area of the nozzle, R specific gas constant and T_0 the stagnation temperature of the combustion chamber. The internal pressure in the chamber is evaluated using the Clapeyron Equation, Eq. (3).

$$P_0 = \rho_{pr} R T_0 \tag{3}$$

where ρ_{pr} is the density of combustion products.

The variation of chamber pressure during the combustion process requires the assessment of mass flow rate through the nozzle. This quantity is a

function of the generated mass rate and the differences in pressures downstream and upstream of the nozzle. The mass flow through the nozzle is equal to the blocked mass if the generated mass is greater than the maximum or the chamber pressure exceed the ambient pressure. According to the De Laval theory, the linear velocity of the exiting exhaust gases is calculated as shown in Eq. (4).

$$v_e = \sqrt{\frac{2kRT_0}{k-1}\left[1-\left(\frac{P_{out}}{P_0}\right)^{\frac{k-1}{k}}\right]} \tag{4}$$

where k is the ratio of specific heats considering biphasic combustion products.

The flow acceleration provided by the nozzle configuration generates the thrust force, Eq. (5). The analytical analysis assumes ideal expansion, with the exit pressure equal to the ambient, so the component that reveals the difference is equal to zero. Figure 3 shows the analytical thrust curve of the motor used in Armação A-22.

$$F = v_e\dot{m} + (P_{out} - P_{atm})A_e \tag{5}$$

with v_e being the flow velocity, $\dot{m}$ the mass flow rate through the nozzle, P_{out} the exit pressure, and P_{atm} the ambient pressure

Considering a De Laval's nozzle, applying the conservation of mass and assuming ideal expansion, Eq. (5) can be rewritten as Eq. (6), Munson *et al.* (2004).

$$F = A_t P_0 \sqrt{\frac{2k^2}{k-1}\left(\frac{2}{k_m+1}\right)^{\frac{k_m+1}{(k_m-1)}}\left[1-\left(\frac{P_{atm}}{P_0}\right)^{\frac{k-1}{k}}\right]} \tag{6}$$

where A_t is the throat area.

MESH CONVERGENCE STUDY

The baseline geometry is a convergent-divergent nozzle, used in Armação A-22 project. The convergent section has a diameter of about 70 mm, a length of about 45 mm and a half-angle of 28.5°, while the divergent section has a diameter of about 50 mm, a length nearly of 70 mm and a half-angle of 12°. Figure 1 shows the nozzle with its dimensions. The fluid domain is 2D-axisymmetric. It considers not only the interior of the nozzle but also the surroundings. The length of the domain after the nozzle exit is about nine times the nozzle length (roughly 1000 mm). In this way, there is room for the shock waves to happen and also accommodate the flow, reducing the influence of the outlet boundary condition. The height of the domain is approximately 250 mm. Figure 2 shows the domain.

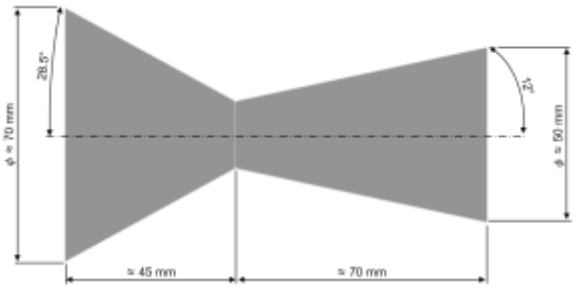

Figure 1. Nozzle dimensions.

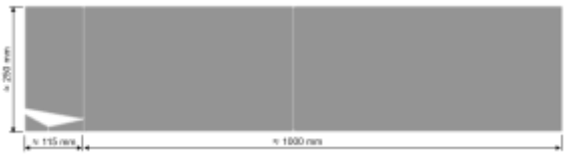

Figure 2. Fluid domain.

The convergence study compares the thrust (the parameter of interest of the present work) to the benchmark results (Table 1). It comprises a combination of mesh refinements and turbulence models, to select the best combination to be used for the other geometries. The meshes are generated using Ansys Meshing, since it can handle 2D geometries. The meshes are entirely made of first order quadrilateral elements and have roughly 139000, 209000, 415400 and 556000 elements. The tested turbulence models are k-ε RNG (Yakhot *et al.* (1992)), k-ω SST (Menter *et al.* (2003)), and Spalart-Allmaras (S-A) (Spalart and Allmaras (1992)).

The thrust curve is a function of time. Due to the unsteady conditions of pressure and mass flow rate, it is not feasible to represent the curve with a single transient simulation. Therefore, the benchmark thrust curve is divided into six operating points. These points have been chosen in such a way the six steady state simulations represent the characteristics of the curve. Figure 3 shows the benchmark curve, with the operating points marked with circles.

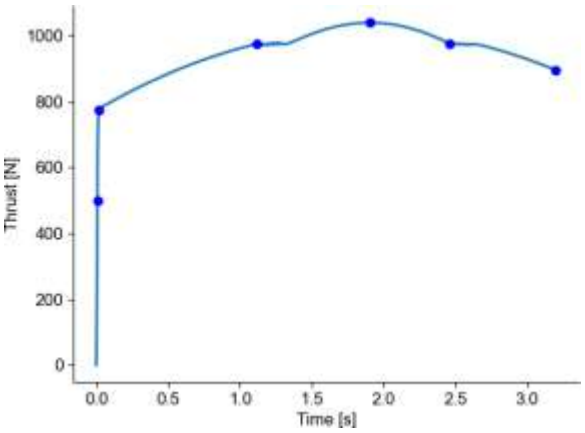

Figure 3. Benchmark thrust curve.

The simulations are pressure-based, with a coupled pressure-velocity scheme, run using Ansys Fluent. The steady- state regime follows a pseudo-transient scheme and runs up to 1000 iterations, with residuals of 1e-3 for continuity, momentum, and turbulence and 1e-6 for energy (by the time continuity residuals reached 1e-3, in most simulations the other residuals were below 1e-7). The walls are modeled as adiabatic and the fluid is taken as ideal gas with constant specific heat (c_p), constant thermal conductivity, viscosity following Sutherland's law. These properties and the molecularweight are based on the MATLAB results, in which the mixture and the particles are converted into equivalent values for a single-phase fluid flow. Table 1 shows the specifications of the operating points. The inlet boundary conditions are taken as mass flow rate and pressure, at a total temperature of 1625 K. The outlet is at atmospheric pressure (101.325 kPa) andambient temperature (293 K).

Table 1. Operating points.

Operating point	Time, s	Inlet mass flow rate, kg/s	Inlet pressure, MPa	Benchmark thrust, N
1	0.0072	0.2823	1.4489	500.7
2	0.0200	0.6611	2.1090	775.5
3	1.1216	0.8161	2.5726	974.4
4	1.9060	0.8657	2.7219	1039.4
5	2.4636	0.8176	2.5755	975.7
6	3.2019	0.7562	2.3896	895.4

Figure 4 shows the results of the convergence study, comparing the thrust relative error between the simulation and the benchmark (MATLAB). Note that the first operating point is not displayed, since it did not converge in most of the simulations or they had large errors. One possible explanation is that this point is not properly represented in MATLAB,since it is placed on a very early transient state of the thrust curve, on the steepest spot of the curve. Therefore, this operating point will not be considered for the rest of the work.

The 139000-element mesh had large errors, regardless of the turbulence model. This was expected to happen since it had issues with the continuity residuals. The 415400 and the 556000-element meshes under the k-ε RNG turbulence model had frequent stabilization issues that delayed considerably the simulations and, for this reason, they were interrupted. Table 2 shows the results in terms of average error and standard deviation, neglecting the first operating point.

The chosen mesh is the 415400-element with Spalart-Allmaras turbulence model, that had the lowest average error and standard deviation. In this way, it is the option that represents best the benchmark curve, with the lowest oscillation from point topoint.

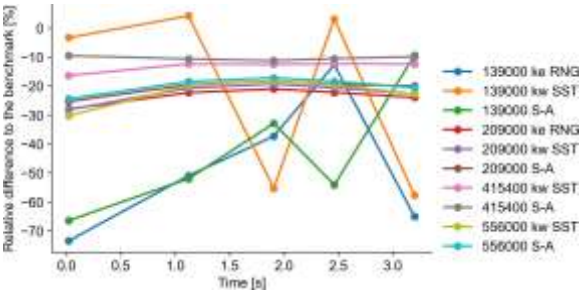

Figure 4. Thrust as relative difference to the benchmark.

Table 2. Convergence study compared to the benchmark, considering operating points 2 to 6.

Mesh	Turbulence model	Average error in magnitude, %	Standard deviation, %
139000	k-ε RNG	47.91	21.51
139000	k-ω SST	24.75	28.48
139000	Spalart-Allmaras	42.99	19.93
209000	k-ε RNG	23.50	2.43
209000	k-ω SST	22.32	3.13
209000	Spalart-Allmaras	20.53	2.49
415400	k-ε RNG	-	-
415400	k-ω SST	13.22	1.61
415400	Spalart-Allmaras	10.37	0.59
556000	k-ε RNG	-	-
556000	k-ω SST	22.16	4.30
556000	Spalart-Allmaras	19.80	2.55

Furthermore, the chosen mesh captures well the boundary layer effects, as the average y+ on the nozzle wall (post- processed using Ansys CFD-Post) is less than 0.16. In terms of average Mach number at the nozzle exit, it is 2.74 for all operating points, except the first one, which is 1.58. Figure 5 shows

the Mach number contours for all operating points. Apart from the first operating point, the other five are very similar.

RESULTS AND DISCUSSION

The new geometries are obtained varying either the divergent or the convergent angle of the nozzle. The change in angle implies either a change in the length or in the diameter of the corresponding section. For the convergent section, it is not possible to change the diameter, due to the communication between fuel chamber and nozzle. For the divergent section, on the other hand, there is no such limitation. The baseline convergent half-angle is 28.5° and the variations consider 27.5°, 28°, 29° and 29.5°. Conversely, the baseline divergent half-angle is 12° and the variations consider 11°, 11.5°, 12.5° and 13°. Therefore, there are twelve new geometries: four with different convergent angle, four with different divergent angle and different divergent diameter, and four with different divergent angle and different divergent length.

Figure 6 shows the thrust curves for all simulation. It is good to show their shape, however, the results should be plotted as relative differences to the baseline to draw a point to point comparison. Therefore, Figure 7 shows the thrust as relative difference to the baseline. The plots are segregated according to the family of geometries. As previously mentioned, the convergent angle of the baseline geometry is based on Mir *et al.* (2017). In their work, the thrust obtained considering this angle as 28°, 28.2°, 28.3°, 29°, 29.5° and 30° follows a slight increase. However, for 28.5° there is a peak. Conversely, the results of the present research shows a similar trend for a convergent angle of 27.5°, 28.5° (baseline), 29° and 29.5°. The peak is observed for 28°. Note that this is not the same angle as Mir *et al.* (2017). In addition, the difference observed

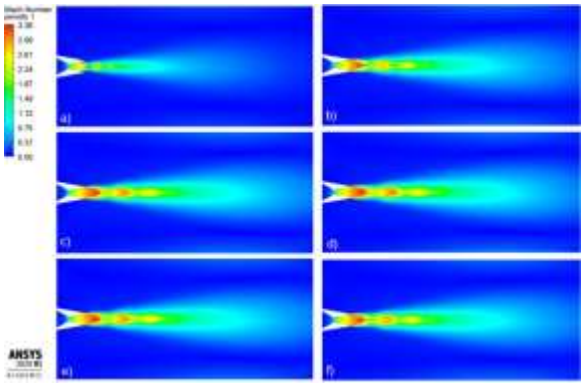

Figure 5. Mach number contours for the baseline. Operating points 1 to 6 represented from a) to f), respectively.

in the present work is larger in relative terms but smaller in terms of order of magnitude. In other words, the thrust varied approximately 40% (or less than 400 N), while Mir *et al.* (2017) shows about 0.5% change (or more than 10000 N).

Concerning the geometries with changes in the divergent angle but with the same exit diameter (i.e. same expansion ratio), all results perform better than the baseline. Note that the results for 11.5°, 12.5° and 13° have a positive concavity, with a smaller difference to the baseline happening at the highest thrust situation (fourth operating point). On the other hand, the results for 11° have negative concavity, but still with all points performing better than the baseline. This reversed trend suggests that there is an optimum value for this angle.

At last, for the geometries with changes in the divergent angle but keeping the same divergent section length (i.e. changing the exit diameter and, consequently, changing the expansion ratio) perform worse than the baseline, except the 11.5° design, that is virtually equal to the baseline (it performs only 0.4% to 0.9% worse than the baseline). In addition, this family of geometries may have an optimum: from 11° to 11.5°, the performance increases; from 11.5° to 12° (baseline), it is almost the same; from 12° (baseline) to 12.5°, it decreases; the exception is from 12.5° to 13°, as it increases for most points.

By treating the variables as relative changes compared to the baseline, the results overrule the segregation by operating points. In other words, the dispersion plots and correlations shown in Figure 8 treat all data equally and are not shaped like a thrust curve. Furthermore, this enables to include other operating points or other geometries in future studies. There are many correlation coefficients available and their use assumes a prior suitability investigation. The most known correlation coefficients are Pearson's r coefficient and Spearman's ρ coefficient. The Pearson's r coefficient assumes a normal distribution. Its hypotheses are strong and more difficult to accomplish. The Spearman's ρ coefficient, on the other hand, does not assume a normal distribution. It is a rank coefficient and performs well for monotonic relations.

The way of testing their suitability is via the p-value test. If the p-value is below the significance value of 5% ($\alpha = 0.05$), it means that there is at least a 95% confidence level that the variables are not non-correlated. Note that each function has its p-value test with different definitions and they be checked in the source code of their correspondent

SciPyfunction (SciPy (2021a), SciPy (2021b)). The p-value test using Pearson's r coefficient yields 0.058 and 1.125e-5 for correlations between thrust and exit velocity, and thrust and exit static pressure, respectively. Since 0.058 is greater thanα, Pearson's r coefficient cannot be used for the first correlation. In order to use the same correlation, Spearman's ρ coefficient is used, as its p-value tests yield 1.22e-27 and 5.02e-10, respectively.

The coefficients are annotated in the bottom of Figure 8. Thrust and exit velocity are extremely correlated (+89%) while thrust and exit static pressure are strongly correlated (-63.3%), but not as high as the first case. Note that the

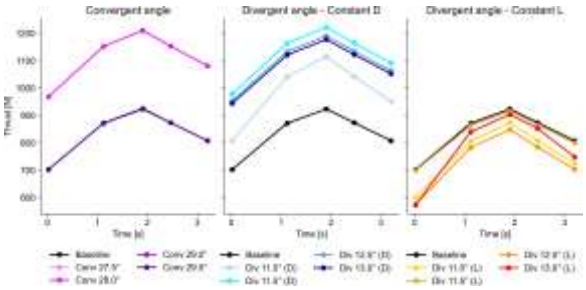

Figure 6. Thrust curves for all simulations.

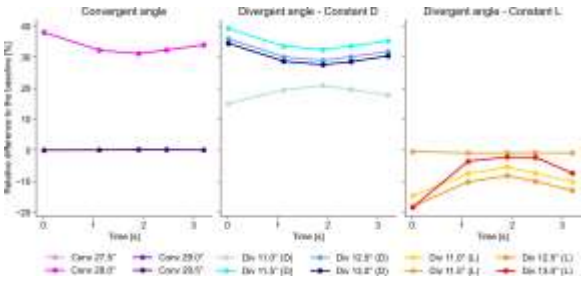

Figure 7. Thrust as relative difference to the baseline.

positive sign means that a positive variation in exit velocity leads to a positive variation in thrust. On the other hand, a negative sign means that a positive variation in exit static pressure leads to a negative variation in thrust. However, Eq. (5) shows that both exit velocity and exit static pressure positively contribute to the thrust. Therefore, by looking into the variations of these parameters, it is clear that an increase in exit velocity overcompensates a decrease in exit static pressure. Furthermore, for an isentropic flow, the total pressure does not change. In other words, the designs that generate more thrust are closely related to higher levels of dynamic pressure (i.e. velocity), which yields a reduction of static pressure to result in the same total pressure.

CONCLUSION

The present research showed the influences of the angles of a convergent-divergent nozzle on the thrust. It simulated the current nozzle design that was based on the literature and twelve modified designs, varying the convergent and the divergent angles by -1.0°, -0.5°, +0.5° and +1.0°. For the convergent section, the variations kept the same convergent diameter, while the divergent section kept the same divergent diameter or the same divergent length. The simulations

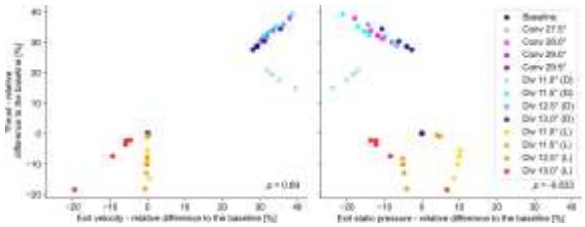

Figure 8. Changes in thrust correlated to changes in exit velocity and exit static pressure.

considered a 2D-axisymmetric domain, with mesh and turbulence model determined after a convergence study, comparing the thrust to a benchmark (MATLAB).

Concerning the convergent angle, the present research showed that a half-angle of 28° produced a peak value for thrust, while the other angles produced similar results. Although this angle does not match 28.5° cited by the literature, this peak behavior happened in both works. For the divergent angle with constant exit diameter, all geometries performed better than the baseline and a half-angle of 11.5° produced the best results for this family. For the divergent angle with constant divergent length, all geometries performed worse than the baseline but a half-angle of 11.5° produced results very similarto the baseline.

The dispersion plots pointed out correlations between thrust and exit velocity, and between thrust and exit static pressure, Figure 8. These plots and the correlation coefficients showed that the designs that increase the velocity, increase the dynamic pressure and, therefore, decrease the static pressure (as the total pressure does not change) generate more thrust. Although correlation does not mean causation, this reasoning based on the physics does bridge the gap and proves a valid cause for the increase in thrust. Therefore, this work showed that the nozzle design should prioritize the conversion of static pressure into dynamic pressure to increase thrust.

The fact that some results produced peak values and some others produced values close to the baseline could be better understood in future works by varying less the angles (instead of 0.5°, 0.1°, for example). Also, more operating points could be added to see improve the discretization of the benchmark thrust curve. In addition, it remains to

be seen if the best results are possible to be combined into a single design or if the combinations lead to totally different results. Besides, the best results still need to be checked concerning the mass distribution of the rocket and if the changes do not affect theflight stability.

ACKNOWLEDGEMENTS

The authors appreciate the sponsorship of SolidWorks, Ansys Inc. and Engineering Simulation and Scientific Software (ESSS) for providing the software used during the development of this research.

REFERENCES

Biju Kuttan, P. and Sajesh, M., 2013. "Optimization of divergent angle of a rocket engine nozzle using computational fluid dynamics". *The International Journal Of Engineering And Science (IJES)*, Vol. 2, No. 2, pp. 196–207.

Hamedi-Estakhrsar, M.H., Mahdavy-Moghaddam, H. and Jahromi, M., 2018. "Investigation of effects of convergence and divergence half-angles on the performance of a nozzle for different operating conditions". *Journal of the Brazilian Society of Mechanical Sciences and Engineering*.

Menter, F.R., Kuntz, M. and Langtry, R., 2003. "Ten years of industrial experience with the sst turbulence model".

Turbulence, Heat and Mass Transfer, Vol. 4.

Miller, W.H., 1971. *Solid rocket motor performance analysis and prediction*, Vol. 8039. National Aeronautics and Space Administration.

Mir, I., Samo, S., Hussain, T., Ali, I. and Durani, H.A.K., 2017. "Influence of convergent section length and angle on performance of supersonic nozzle". *Sindh University Research Journal (Science Series)*, Vol. 49, No. 004, pp. 727–732.

Munson, B.R., Young, F. and Okiishi, T.H., 2004. *Fundamentals of fluid mechanics (in portuguese)*. Editora Blucher. Natta, P., Kumar, V.R. and Rao, Y.V.H., 2012. "Flow analysis of rocket nozzle using computational fluid dynamics (cfd)".

Engineering Research and Applications (IJERA), Vol. 2, No. 5, pp. 1226–1235.

Noh, M.H.M., Hamid, A.H.A., Atan, R. and Rashid, H., 2011. "Numerical investigation of chocked converging-divergingnozzles for thruster application". *IIUM Engineering Journal*, Vol. Special Issue, Mechanical Engineering.

SciPy, 2021a. "scipy.stats.pearsonr". SciPy v1.6.3 Reference Guide, docs.scipy.org/doc/scipy/reference/generated/scipy.stats.pearsonr.html. Accessed in 15/06/2021.

SciPy, 2021b. "scipy.stats.spearmanr". SciPy v1.6.3 Reference Guide, docs.scipy.org/doc/scipy/reference/generated/scipy.stats.spearmanr.html. Accessed in 15/06/2021.

Spalart, P.R. and Allmaras, S.R., 1992. "A one-equation turbulence model for aerodynamic flows". *AIAA*, Vol. 30. Sutton, G.P. and Biblarz, O., 2016. *Rocket propulsion elements*. John Wiley & Sons.

Yakhot, V., Orszag, S.A., Thangam, S., Gatski, T.B. and Speziale, C.G., 1992. "Development of turbulence models forshear flows by a double expansion technique". *Physics of Fluids A*, Vol. 4, No. 7, pp. 1510–1520.